Seismic analysis of masonry arches

S. De Santis & G. de Felice
Roma Tre University, Department of Structures, Rome, Italy

SUMMARY:
Masonry arches and vaults have demonstrated to be one of the critical elements in the seismic vulnerability of historic constructions. Their dynamic behaviour is generally described by recurring to the mechanism method or, as an alternative, to 3D finite elements and macro-elements. More research is however needed to develop reliable seismic assessment methods. In the current paper a modelling approach which makes use of fibre beam elements is proposed. The seismic capacity of masonry arches is assessed through cyclic push-over analyses under different load distributions and compared to incremental dynamic analyses under natural accelerograms to indentify an adequate representation of inertial forces. Then, the presence of pillars and strengthening devices, such as steel tie-bars and externally bonded composite material strips, is considered to investigate their influence on the seismic capacity.

Keywords: Masonry arches; Seismic analysis; Seismic retrofitting

1. INTRODUCTION

Damage and collapses caused by earthquakes show that masonry arches and vaults are one of the most vulnerable elements in historic constructions. Nevertheless, a deep knowledge of their dynamic behaviour is still lacking and, to date, only a few scientific papers have been addressed to their seismic assessment. Also, analysis tools shared by researchers and practising engineers are needed, leading to reliable results and ensuring at the same time the computational sustainability. As a consequence, the seismic assessment of masonry arches and vaults is generally affected by so many uncertainties that drastic provisions of substitution or of invasive and indiscriminate strengthening are often adopted in the retrofitting of historic buildings.
As regards the scientific research on the subject, the dynamic behaviour of masonry arches is usually studied through the mechanism method (Oppenheim, 1992; Clemente, 1998; De Luca et al., 2004), based on Heyman's assumptions (1966) of infinite compressive strength and no tensile resistance. The method is suitable for elegant analytical solutions and leads to a rough estimate of the seismic capacity of the arch as the horizontal load resultant causing the development of four plastic hinges, inducing in turn the activation of the arch collapse mechanism. The results of the mechanism method have also been used to validate numerical simulations performed using distinct elements (DeJong and Ochsendorf, 2006; De Lorenzis et al., 2007a), which describes the structure as an assemblage of rigid blocks and non linear interfaces and allows its dynamic response to be accurately modelled. The Distinct Element Method is however inadequate for the study of large three-dimensional structures made out of a large number of elements.
As further alternatives, 2D and 3D finite elements (Pelà et al., 2009) or 1D macro-elements (Resemini and Lagomarsino, 2007) can be used to assess the seismic capacity of masonry arches according to the performance based approach suggested by the most recent scientific papers (Lagomarsino and Resemini, 2009) and advanced standards on the protection of the cultural heritage (Ministero per i beni e le attività culturali, 2010). On the one hand, 3D models allow the geometry of all the structural elements to be faithfully reproduced, but the computational effort they ask for is generally prohibitive. On the other hand, even if onerous non linear dynamic analyses can be made using macro-elements, it

can be relatively difficult to represent the actual conformation of the structure and the interaction between axial force and bending moment in its elements.
Dynamic testing appears particularly promising to develop a deeper understanding of the response of masonry arches and vaults and validate numerical simulations. Only few studies have however been carried out in the last decade, mainly addressed at demonstrating the effectiveness of strengthening or restoration techniques (Barbieri and Di Tommaso, 2003; Barbieri et al., 2002; Ceradini and Tocci, 2004) or at performing structural identification and parameter calibration of elastic FE models (Conte et al, 2011). One of the most challenging issues in field dynamic testing is the dynamic excitation. An impact hammer (Atamturkur et al., 2007; Ceradini and Tocci, 2004) or a vibrodyne (Barbieri et al., 2002) have been often used. Free vibrations starting from an initial deformed configuration are instead investigated in (Barbieri and Di Tommaso, 2003).
The dynamic response of masonry vaults is studied in the current paper through a modelling strategy based on the use of fibre beam elements. Cyclic push-over and incremental non-linear dynamic analyses are performed on circular arches to identify an adequate representation of the inertial forces arising during earthquake excitation. Then, the presence of pillars is included to study its effect on the seismic capacity. Finally, the improvement provided by different strengthening devices, such as tie-bars and externally bonded composite material strips, is evaluated.

2. MODELLING APPROACH

Starting from experimental results showing that plane sections remain plane after deformation (de Felice and De Santis, 2010), masonry elements under compression and bending can be represented through 1D models. Fibre beam elements are used in the current work, which have already been used to evaluate the load carrying capability of masonry bridges (de Felice, 2009) and study the dynamics of arches under pulse base accelerations (De Santis, 2011).
According to the proposed modelling strategy, a masonry arch is represented as a segmental beam, made out of flexibility based frame elements with fibre cross section. The method allows accurate analyses under complex loading histories to be performed, ensuring at the same time low computational costs thanks to the intrinsic simplicity of a 1D element and to the discretisation of the cross section into fibres. Uniaxial relations are assigned to the fibres and the actual behaviour of the material is accounted for, including the post-peak deterioration and the hysteretic response revealed by laboratory studies carried out by the authors on brickwork prisms under compression and bending (de Felice and De Santis, 2010). In the present case, the Kent&Park (1971) law represented in Figure 1 is used.

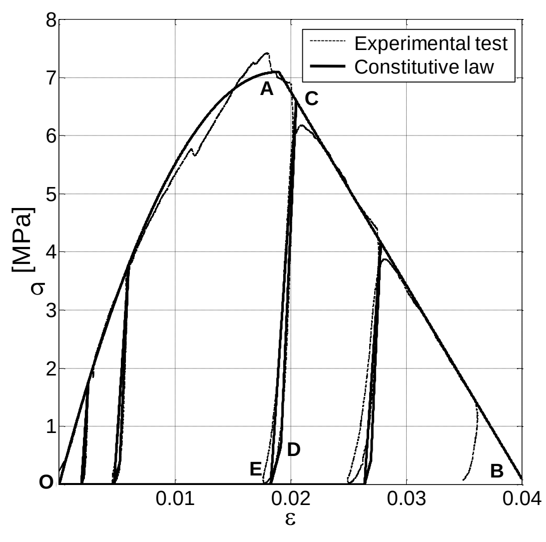

Figure 1. Experimental stress-strain curve for a brickwork prism under cyclic compression and uniaxial constitutive relation adopted in numerical simulations (compressive stresses are assumed as positive).

The skeleton curve (OAB) consists of an ascending parabolic branch followed by a linear softening phase with no residual strength. Based on laboratory studies, a compressive strength of 7MPa, 700MPa initial stiffness and deterioration rate (ratio between ultimate strain and peak strain) equal to 2.2 are assumed in compression, while the tensile strength is neglected. The cyclic response is also accurately described, by bi-linear unloading branches (CDE) and linear reloading braches (EC) so as to reproduce the experimental curve (Figure 1).
The arch is modelled by means of 100 non linear fibre beam elements each, having the cross section divided into 80 fibres in the bending direction. The backfill and the fill soil are not included in the simulations. Finally, the piers, when present, are made out of 10 fibre beams, whose cross section is divided into 40 fibres.

3. SEISMIC ASSESSMENT THROUGH CYCLIC PUSH-OVER AND INCREMENTAL DYNAMIC ANALYSES

3.1. Cyclic push-over analyses

Aiming at investigating the seismic response of masonry arches under earthquake motion, push-over analyses and non-linear dynamic (step-integration) analyses are performed on a single arch with radius R=10m, thickness s=0.15R and angle of embrace β=157.5°.
The following three different load distributions are used in push-over analyses:

- #1: horizontal loads proportional to nodal masses;
- #2: horizontal loads proportional to the product of masses and horizontal components of first mode displacements;
- #3: horizontal and vertical loads, proportional to the product of masses and first mode displacements. Distribution #3 accounts for the presence of non-null displacement components in both vertical and horizontal directions in the modal shape.

The resulting three capacity curves are shown in Figure 2. The horizontal displacement of the key node (d_k) and the resultant base shear divided by the arch self weight (V_b/W) are assumed as the structure state variables and are on the x-axis and y-axis, respectively. Since the arch is symmetric, the capacity curves are also symmetric. Different load distributions lead to significantly different strength values: passing from distribution #1 to #2 and #3 the ultimate load (maximum V_b) reduces from ca. 33%, to 28% and 21% W. The initial stiffness, instead, remains relatively unchanged. The narrow cycles indicate a low hysteretic dissipation due to cyclic loading, which is similar to the response of a rigid block in rocking motion, confirming that masonry arches behave as rigid body systems under the same (simplifying) constitutive assumptions, as pointed out also in (Lagomarsino and Resemini, 2009).

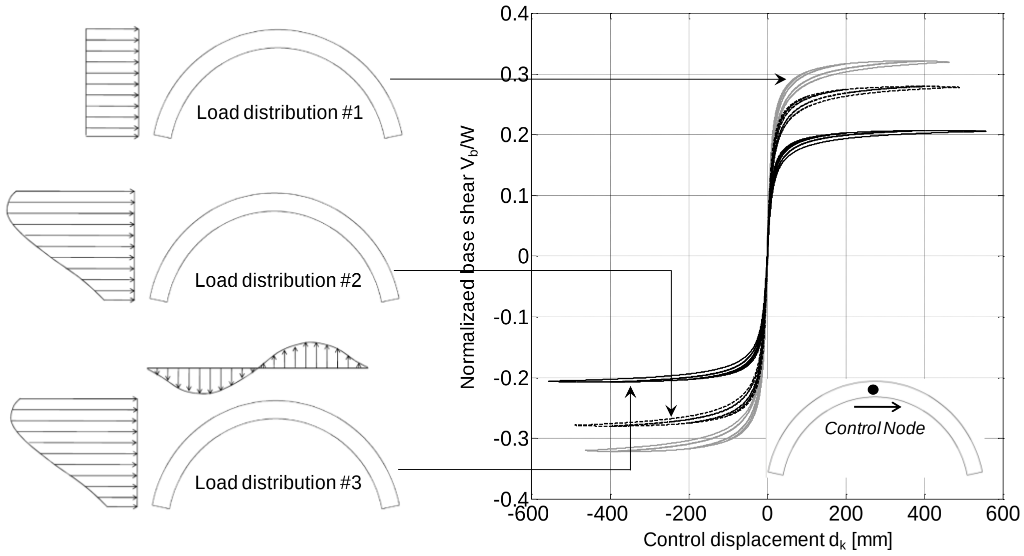

Figure 2. Cyclic push-over curves under different load distributions on an arch with R=10m, s=0.15R, β=157.5°.

3.2. Incremental non-linear dynamic analyses (IDA)

Non-linear dynamic analyses are performed under a set of 14 natural accelerograms selected from the European Strong Motion Database (ESD) so that their average response spectrum matches the synthetic spectrum provided by Eurocode 8 (CEN, 2003) assuming 0.15g PGA and soil B. The signals have 0.86g average peak acceleration and are recorded from events with moment magnitude between 5.6 and 6.9, on recording stations at least 20km far from the source. Weak events and near filed registrations are therefore avoided. In the selection process, performed using Rexel software (Iervolino et al., 2009a), signals are scaled to achieve a maximum spread from the target spectrum of ±10% in the 0.15-2.50sec range. A maximum average scaling factor of 5 and a maximum single scaling factor of 10 are chosen to be applied on the acceleration axis. If more compliant sets are found, the one having the lowest variability is chosen to restrict record-to-record dispersion of the structural response (Iervolino et al., 2009b).

In the fibre beam model, the damping is represented by means of a Rayleigh viscous term. Since hysteretic damping is already included through the material constitutive law, Rayleigh damping represents the dissipative effects induced by other phenomena which are not explicitly described, such as local inelastic deformations due to inhomogeneous stress distribution at the micro-scale that can also occur in a range of average macroscopic stresses that are well below the elastic threshold.

The equivalent viscous damping ratio to be used in dynamic analyses on masonry structures is a particularly challenging issue. Some proposals have been made on the base of shaking table tests in (Benedetti et al., 1998; Juhásová et al., 2008; Mazzon et al., 2009; Elmenshawi et al., 2010). Values ranging from 2% to 10% are suggested, even if in all these works only walls or small-scale building models are considered. Moreover, higher damping ratios should be used for severe earthquake scenarios (ultimate limit state condition), for which strong damage is expected, and for prevalence of flexural response, while lower values should be assumed when weak events (serviceability limit state condition) are studied and the shear is expected to mainly govern the structural response.

The damping parameters are chosen to achieve an equivalent damping ratio of 2% at the first and fourth modal frequencies (f_1=2.25Hz and f_4=8.40Hz). As for the chosen value, 2% appears reasonable by looking at the cyclic capacity curves and considering that neither fill soil nor spandrel walls are included in the structure. As for the frequencies at which damping is fixed, they are related to the highest participating masses in horizontal direction. Damping results to be reasonable within the range of the significant frequencies (in terms of spectral content) of both the input signal and the structural response. High damping values are instead accepted for very low frequencies (<0.2Hz), which are usually reset to zero in the filtering process of sampled recorded signals, as well as for high frequencies (>50Hz), which can result from numerical instabilities and, anyway, have negligible importance in terms of structural dynamic response.

Input signals are applied with increasing scaling factor (SF) ranging from 0.1 to 3.0. The whole response curves of two simulations (having SF equal to 0.8 and 1.2) under two signals included in the set are shown in Figure 3 as sake of example. They result to be close to the capacity curve of the push-over analysis, provided that distribution #3 is adopted.

During non-linear dynamic analyses one or more structural state variables have to be monitored and three choices can be made to synthetically represent the overall response and to make comparisons with static methods: the maximum displacement of the control node and the corresponding (same time instant) resultant base shear; the maximum base shear and the corresponding displacement of the control node; the maximum displacement and the maximum resultant base shear within a time window (having a given amplitude) centred in the time instant of maximum displacement (Ferracuti et al., 2008). When dealing with potentially deteriorating systems (showing a softening branch in the global static load-displacement curve) the first choice is preferable with respect to the second one. The last option has instead a uncertain mechanical justification, unless it is intended as a way to account for higher modes having a non-negligible influence on the dynamic response of a MDOF system. In the current work, the maximum horizontal displacement of the crown (d_k) and the corresponding (same instant) normalized resultant base shear (V_b/W) are chosen as structure state variables and are used to make comparisons with push-over analyses.

The set of dots from all the simulations results to be widely scattered (Figure 4) due to the variability of the signal properties as well as of the structural response. The average IDA curve is derived and a good agreement is found between static and dynamic approaches provided that both horizontal and vertical loads proportional to the product of masses and modal displacements is applied in push-over analyses (load distribution #3). Therefore, this is likely to be an adequate representation of the inertial forces arising in the actual dynamic response of the arch.

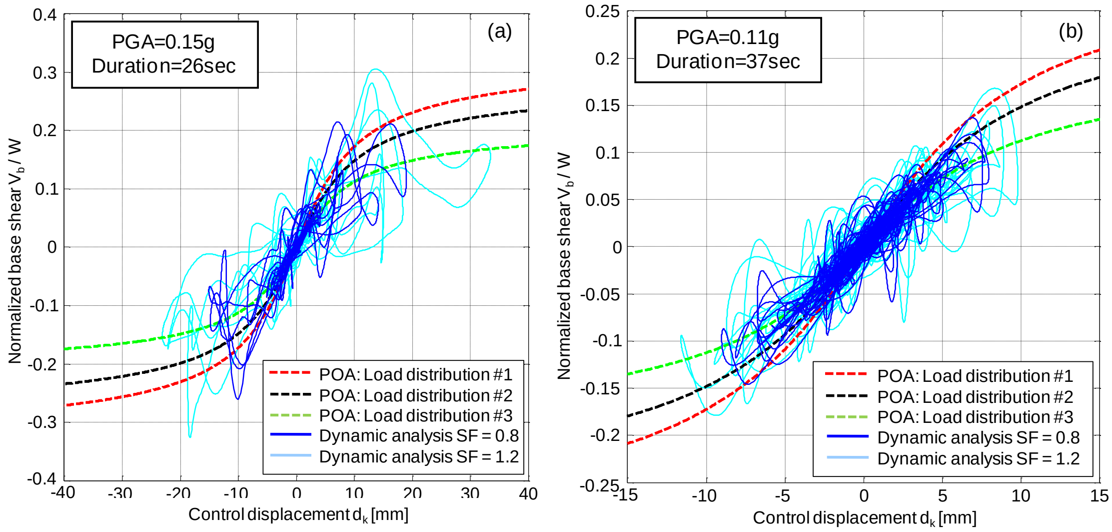

Figure 3. Comparison between push-over and non-linear dynamic analyses under two accelerograms from the set: response curves of two dynamic simulations with different scaling factors (SF).

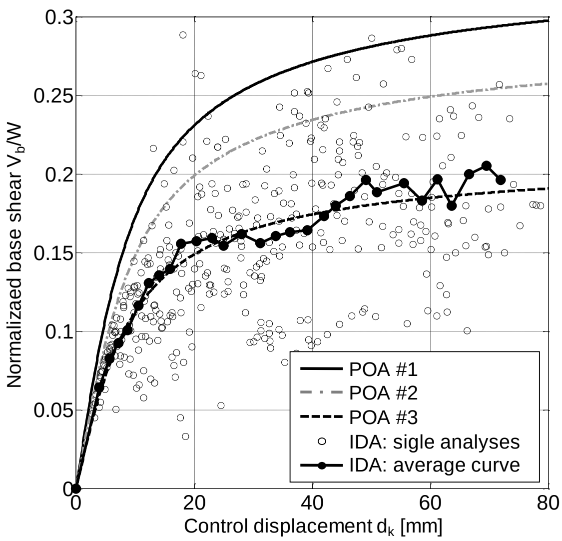

Figure 4. Average IDA curve and push-over curves for different load distributions on a circular arch with R=10m, s/R=0.15, β=157.5°.

4. ARCHES ON PILLARS AND STRENGTHENED ARCHES

Push-over analyses are carried out on arches built on pillars to investigate how the seismic capacity changes when the springers are allowed to move with respect to each other. The arch is the same as the one considered in the previous section (R=10m, s/R=0.15, β=157.5°) and the pillars are identical so the structure is symmetric. The applied load configuration is proportional to the product of masses and first mode displacements including both horizontal and vertical forces (distribution #3). Clearly, the load distribution slightly changes depending on the pillar size as the modal shape changes (Figure 5). On the one hand, the loads on large piers become predominant with respect to the loads on the arch because of the heavy masses; on the other hand, the more slender are the pillars, the higher are the horizontal displacements with respect to the vertical displacements. Accordingly, the horizontal loads adopted in push-over analyses become predominant with respect to the vertical loads. Assuming that the modal shape is a reliable representation of the structural displacement field under earthquake motion, such variations account for the filter effect on the seismic action applied on the arch springers produced by the pillars, as it is requested by recent standard codes for the evaluation of the seismic demand within the analysis of local mechanisms involving limited portions of the structures that are not directly based on the foundation but are instead placed in high (Ministero delle infrastrutture, 2009).

The ultimate load is obtained for numerous values of the pillar slenderness, defined as the ratio between its height (h) and its width (d); by doing so the two effects of the pillar shape (h/d) and of the pillar size (d) are investigated. Four width values ranging from 2m to 5m are considered, which are reasonable given the arch size. The normalized seismic capacity (V_b/W) obtained on the structure made out of arch and pillars is divided by the normalized capacity of the arch alone (V_{b0}/W) to get a better representation of the strength reduction due to the presence of the piers.

Structures with very squat piers behave analogously to the arch without pillars (Figure 5) since the collapse mechanism does not involve the pillars (local mechanism, M0). The seismic capacity does not change, remaining the same as for the arch alone, until a limit slenderness is reached. Above this value the collapse mechanism changes and involves one pillar, but the other pillar is never involved (semi-global mechanism, M1). The resistance towards seismic actions reduces with the slenderness increase until, if the pillars are very slender, the structure is not even able to sustain its self weight. The change of the mechanism occurs for different slenderness limit values depending on the pier width and ranging from 0.4 (d=2m) to 1.8 (d=5m).

When the collapse mechanism is local or semi-global, the seismic capacity is derived as the horizontal maximum load applied on the portion of the structure that is actually involved in the mechanism divided by its self-weight. It is also worth saying that the failure mode is obtained from push-over simulations, whose duration is in the order of ten seconds, and no preliminary analyses are necessary to identify the positions of the hinges. The failure modes are represented in Figure 5 similarly to rigid block collapse mechanisms as sake of simplicity. Actually, due to the assumed constitutive assumptions (accounting for finite crushing strength and post-peak deterioration), and to the continuum nature of the finite element approach, no concentrated hinges but portions of distributed inelastic deformations are obtained.

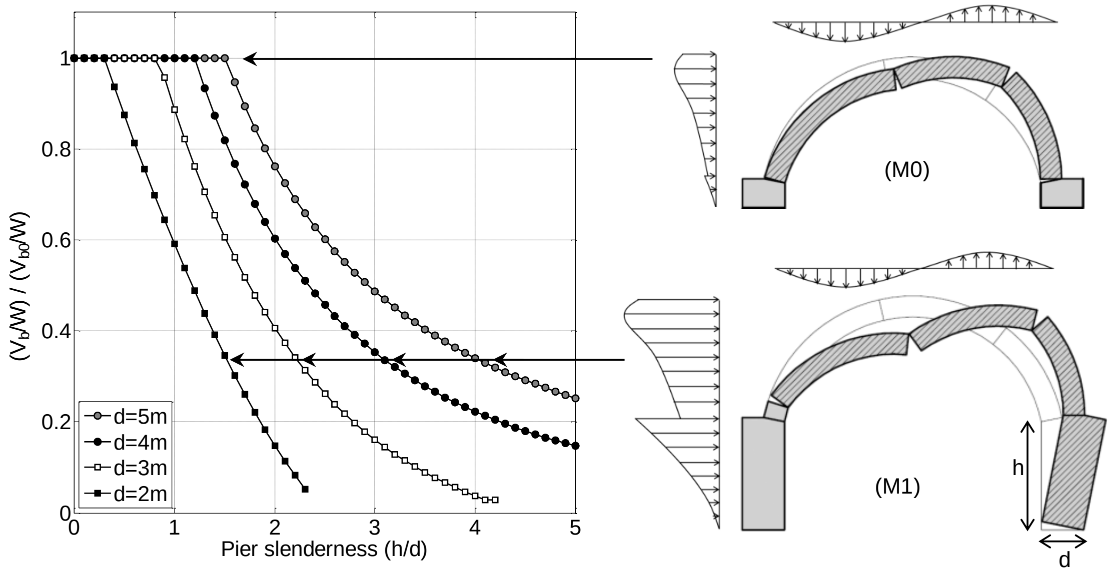

Figure 5. Seismic capacity of arches on pillars vs. pillar slenderness for different values of pillar width.

The introduction of steel tie-bars represents one of the most diffused strengthening techniques to improve the structural behaviour of an arch towards both vertical and seismic actions, since it sustains the horizontal thrust at the springers and constrains their relative movement. Recently, externally bonded strips of composite materials, such as FRP and SRG, have also been widely adopted to retrofit existing structures; applications to masonry arches are reported, among others, in (Foraboschi, 2004; De Lorenzis et al., 2007b; Drosopoulos et al., 2007). The effectiveness of the two strengthening approaches when applied, separately or together, on masonry arches built on pillars is investigated in this section of the paper.

Pillars have 3m width and 7.5m height (slenderness h/d=2.5), while the arch is the same of previous sections (R=10m, s/R=0.15, β=157.5°). The steel tie-bar is modelled as a truss element connecting the tops of the piers and having the cross section area of a ∅30 cylindrical rod. It resists only in tension, with an elasto-plastic law having a yielding stress of 230MPa. Due to the buckling, its contribution in compression is instead neglected (Figure 6). The composite strip is included by changing the mechanical properties of one fibre in the cross section of the arch at the extrados level. The constitutive relation assigned to the new fibre is elasto-fragile in tension and non resistant in compression as the externally bonded strip does not provide any stiffness or resistance when compressed. Since the fibre beam model adopted in the present work is based on the plane section assumption, the fibres are not allowed to slide with respect to each other. Therefore, the debonding failure of externally bonded materials cannot be represented. Such a failure mode is however prevented by the arch curvature when the strengthening layer is applied on the extrados, like in the present case. As for the tensile strength of the bonded strip, it is generally much higher than the actual stress induced in the strengthening layer, which is rather designed to achieve a well distributed influence on the arch extrados.

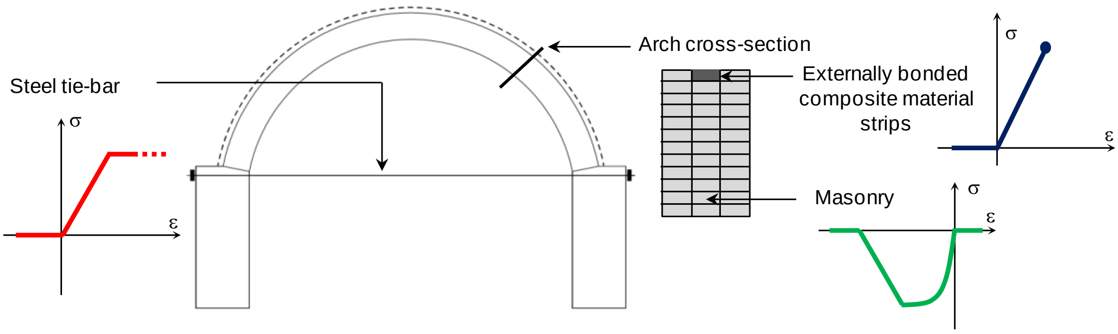

Figure 6. Modelling of strengthened arches on pillars.

Push-over analyses under load distribution #3 are performed to study the structural performance under seismic actions. The resulting capacity curves are represented in Figure 7 together with the collapse mechanisms activated on the different structure configurations. The control displacement is the horizontal translation of the key node, while the capacity is defined as the ratio between the maximum horizontal load and the self weight of the portion of the structure which is actually involved in the mechanism.

The first configuration is the unreinforced arch, showing a semi-global collapse mechanism (M1) characterised by the development of three hinges on the arch and a fourth hinge at the base of one pier; the seismic capacity of the unstrengthened structure is ca. 0.07W. The introduction of a steel tie-bar produces an increase in the resistance towards seismic loads up to ca. 0.14W (twice the arch with no reinforcement) and a change in the failure mode which becomes a global mechanism (M2) since the tops of the piers cannot move away from each other. Two hinges develop in the arch (one on the intrados and one on the extrados) and two other hinges develop at the base of the piers. If the strengthening is made by applying externally bonded strips on the arch extrados an even higher capacity is obtained (ca. 0.19W). In this case the collapse mechanism (M3) is semi-global and consists in one hinge close to the top of the left-hand pier, two hinges on the right-hand pier (one on the base and one approximately in the middle) and a fourth hinge on the arch; the arch intrados cracks since the reinforcement layer prevents the crack opening in the extrados. Finally, if the two devices are applied together, the seismic capacity reaches ca. 0.27W (four times the first configuration) and the failure mode changes again (M4). The mechanism is global since the tie-bar makes the piers move together and no cracks can open in the arch extrados due to the reinforcement layer. The hinges are located at the base of the two piers, at mid-height of the right-hand pillar and, finally, on the arch intrados close to the left-hand pillar.

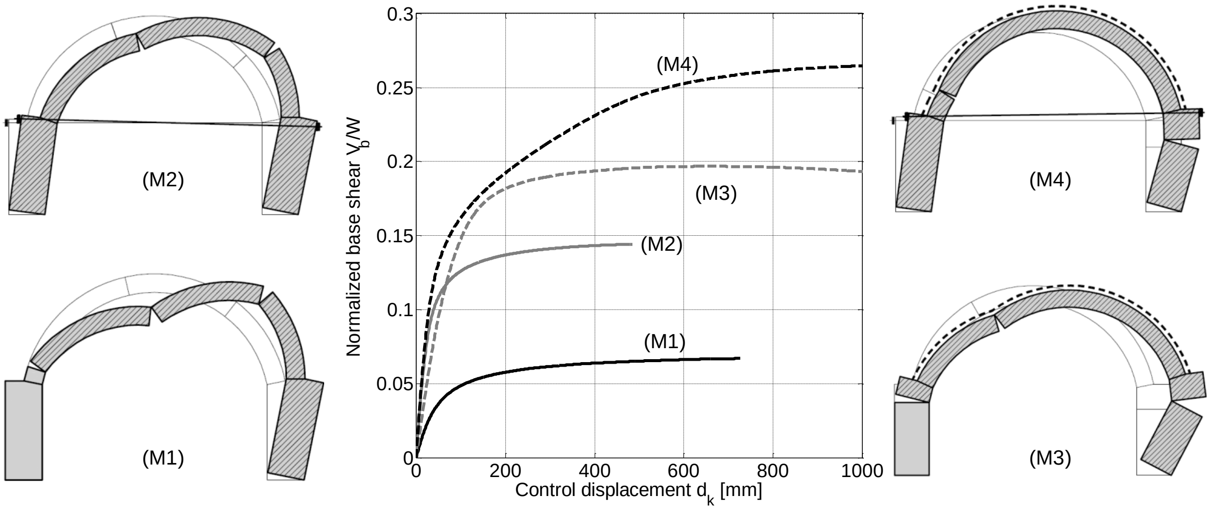

Figure 7. Push-over curves and failure mechanisms for arches on pillars with different strengthening devices: no strengthening (M1), tie-bar (M2), externally bonded composite material strips (M3), and tie-bar and externally bonded composite material strips (M4).

CONCLUSIONS

A modelling approach based on fibre beam elements is used to represent masonry arches under seismic loads. Non-linear dynamic simulations under a set of natural accelerograms are performed on circular arches and compared to push-over analyses revealing that a good agreement is found provided that a load distribution is used that includes both horizontal and vertical loads proportional to the product of masses and first mode displacements, to account for the presence of non-null displacement components in both vertical and horizontal directions in the modal shape. Thus, this appears to be an adequate representation of the inertial forces arising in the actual response of a masonry arch under earthquake motion to be used within push-over based seismic assessment procedures.

Push-over analyses on arches built on pillars show that the seismic capacity decreases with the pier slenderness, except when the pier is so stiff that the collapse mechanisms does not even involve it. The effect of both classical and innovative strengthening techniques, such as steel tie-bars and externally bonded composite material strips applied on the arch extrados, is evaluated. The former prevents the relative movement of the arch springers, while the latter does not allow the crack opening on the arch extrados. As a result, the weakest failure modes are constrained and a significant capacity improvement is achieved.

REFERENCES

Atamturktur, H.S., Hanagan, L.M., Boothby, T.E. (2007). Extension of Large-scale Modal Analysis Techniques to Historic Masonry Vaults. *XXV IMAC Conference*.

Barbieri, A., Borri, A., Corradi, M., Di Tommaso, A. (2002). Dynamic behaviour of masonry vaults repaired with FRP: experimental analysis. *Sixth International Masonry Conference*.

Barbieri, A., Di Tommaso A. (2003). Prove dinamiche su volte in muratura rinforzate con composite. *INARCOS* **636:2**,15-21. [in Italian].

Benedetti, D., Carydis, P., Pezzoli, P. (1998). Shaking table tests on 24 simple masonry buildings. *Earthquake Engineering and Structural Dynamics* **27:1**,67-90.

CEN, European Committee for Standardisation. (2003). EN 1998-1 Eurocode 8: Design Provisions for Earthquake Resistance of Structures, Part 1.1: General rules, seismic actions and rules for buildings.

Ceradini, V., Tocci, C. (2004). Sperimentazione dinamica su volte murarie piane. *XI Congresso ANIDIS*. [in

Italian].
Clemente, P. (1998). Introduction to dynamics of stone arches. *Earthquake Engineering and Structural Dynamics* **27:5**,513-522.
Conte, C., Rainieri, C., Aiello, M.A., Fabbrocino, G. (2011). On-site assessment of masonry vaults: dynamic tests nd numerical analysis. *Geofizika* **28:1**,127-143.
de Felice, G. (2009). Assessment of the load-carrying capacity of multi-span masonry arch bridges using fiber beam elements. *Engineering Structures* **31:8**,1634-1647.
de Felice, G., De Santis, S. (2010). Experimental investigation and numerical modelling of historic brickwork for railway arch bridges assessment. *International Journal of Architectural Heritage* **4:2**,115-137.
De Lorenzis, L., DeJong, M., Ochsendorf, J. (2007a). Failure of masonry arches under impulse base motion. Earthquake *Engineering and Structural Dynamics* **36:14**,2119-2136.
De Lorenzis, L., Dimitri, R., La Tegola, A. (2007b). Reduction of the lateral thrust of masonry arches and vaults with FRP composites. *Construction and Building Materials* **21:7**,1415–1430.
De Luca, A., Giordano, A., Mele, E. (2004). A simplified procedure for assessing the seismic capacity of masonry arches. *Engineering Structures*, **26:13**,1915-1929.
De Santis, S. (2011). Load-carrying capability and seismic assessment of masonry bridges. *PhD Dissertation, Roma Tre University, Rome, Italy*.
DeJong, M., Ochsendorf, J.A. (2006). Analysis of vaulted masonry structures subjected to horizontal ground motion. *5th International Conference on Structural Analysis of Historic Constructions, New Delhi, India*.
Drosopoulos, G.A., Stavroulakis, G.E., Massalas, C.V. (2007). FRP reinforcement of stone arch bridges: Unilateral contact models and limit analysis. *Composites: Part B*, **38:2**,144-151.
Elmenshawi, A., Sorour, M., Mufti, A., Jaeger, L. G., Shrive, N. (2010). Damping mechanisms and damping ratios in vibrating unreinforced stone masonry. Engineering Structures **32:10**,3269-3278.
Ferracuti, B., Pinho, R., Savoia, M. (2008). Statistical validation of nonlinear push-over methods by incremental dynamic analyses. *Valutazione e riduzione della vulnerabilità sismica di edifici esistenti in cemento armato. Polimetrica: Milano, Italy.*
Foraboschi, P. (2004). Strengthening of masonry arches with fiber-reinforced polymer strips. *Journal of Composites for Construction Construction, ASCE*, **8**:3,191-202.
Heyman, J. (1966). The stone skeleton. *International Journal of Solids and Structures*, **2:2**,249-279.
Iervolino, I., Galasso, C., Cosenza, E. (2009a). REXEL: computer aided record selection for code-based seismic structural analysis. *Bulletin of Earthquake Engineering* **8:2,**339-362.
Iervolino, I., Maddaloni, G,. Cosenza, E. (2009b). A note on selection of time-histories for seismic analysis of bridges in Eurocode 8. *Journal of Earthquake Engineering* **13:8**,1125-1152.
Juhásová, E., Sofronie, R., Bairrão, R. (2008). Stone masonry in historical buildings - Ways to increase their resistance and durability. *Engineering Structures* **30:8**,2194-2205.
Kent, D.C., Park, R. (1971). Flexural members with confined concrete. *Journal of the structural division, ASCE*, **97:7**,1969-1990.
Lagormarsino, S., Resemini, S. (2009). The assessment of damage limitation state in the seismic analysis of monumental buildings. *Earthquake Spectra* **25:2**,323-346.
Mazzon, N., Valluzzi, M., Aoki, T., Garbin, E., De Canio, G., Ranieri, N. Modena, C. (2009). Shaking table tests on two multi-leaf stone masonry buildings. *11th Canadian masonry symposium, Toronto, Ontario, Canada*.
Ministero delle infrastrutture. (2009). Istruzioni per l'applicazione delle “Nuove norme tecniche per le costruzioni” (Circolare 02/02/2009), 2009. [Italian Standard, in Italian].
Ministero per i beni e le attività culturali. (2010). Linee Guida per la valutazione e riduzione del rischio sismico del patrimonio culturale allineate alle nuove Norme tecniche per le costruzioni. *Circ. 26 del 2/12/2010*. [Italian Standard, in Italian].
Oppenheim, I.J. (1992). The masonry arch as a four-link mechanism under base motion. *Earthquake Engineering and Structural Dynamics* **21:11**,1005-1017.
Pelà, L., Aprile, A., Benedetti, A. (2009). Seismic assessment of masonry arch bridges. *Engineering Structures* **31:8**,1777-1788.
Resemini, S., Lagormarsino, S. (2007). Displacement-based methods for the seismic assessment of masonry arch bridges. *Fifth International Conference on Arch Bridges ARCH’07*. 441-450.